THE GERONTOLOGICAL SOCIETY OF AMERICA®

Journals of Gerontology: Biological Sciences
cite as: *J Gerontol A Biol Sci Med Sci*, 2017, Vol. 72, No. 9, 1187–1195
doi:10.1093/gerona/glw336
Advance Access publication January 20, 2017

OXFORD

Original Article

Chronic Resveratrol Treatment Inhibits MRC5 Fibroblast SASP-Related Protumoral Effects on Melanoma Cells

Beatrice Menicacci,[1,2] Anna Laurenzana,[1] Anastasia Chillà,[1] Francesca Margheri,[1] Silvia Peppicelli,[1] Elisabetta Tanganelli,[1] Gabriella Fibbi,[1] Lisa Giovannelli,[3] Mario Del Rosso,[1] and Alessandra Mocali[1]

[1]Department of Experimental and Clinical Biomedical Science, Section of Experimental Pathology and Oncology, University of Florence, Italy. [2]Department of Medical Biotechnologies, University of Siena, Italy. [3]Department NeuroFarBa, Section of Pharmacology and Toxicology, University of Florence, Italy.

Address correspondence to Alessandra Mocali, PhD, Department of Experimental and Clinical Biomedical Science, Section of Experimental Pathology and Oncology, University of Florence, Viale G.B. Morgagni 50, 50134 Florence, Italy. E-mail: amocali@unifi.it

Received June 16, 2016; Editorial Decision Date November 26, 2016

Decision Editor: Rafael de Cabo, PhD

Abstract

Cellular senescence is related to organismal aging and is observed after DNA damaging cancer therapies, that induce tumor-suppressive modifications, but it is characterized by a strong increase in secreted factors, termed the "senescence-associated secretory phenotype" (SASP). Particularly, SASP from stroma senescent fibroblasts creates a cancer-favoring microenvironment, providing targets for anti-cancer interventions. In the present article, chronic treatment (5 weeks) with 5 μM resveratrol has been used to modulate senescence-related protumoral features of MRC5 fibroblasts, reducing SASP-related interleukins IL1α, IL1β, IL6, and IL8; transforming-growth-factor-β (TGFβ); matrix metallo-proteinases MMP3 and MMP2; urokinase plasminogen activator (uPA); receptor proteins uPAR, IL6R, insulin growth factor receptor-1 (IGF-1R), TGFβ-R2, and CXCR4. The cellular nuclear-factor-kB (NF-kB) protein level was also reduced, confirming its role in the induction of SASP. Resveratrol pretreated MRC5 fibroblasts were resistant to activation by TGFβ. Resveratrol treatment of senescent MRC5 induced the production of conditioned media (CM) which counteracted the protumoral effect of senescent CM on A375 and A375-M6 melanoma cell proliferation and invasiveness, and reduced the expression of epithelial-to-mesenchymal transition markers related to malignant features. This experimental approach proposes a treatment that targets the senescent stromal cell phenotype to induce an anti-tumor hosting microenvironment, which is suitable for both preventive and therapeutic purposes.

Keywords: resveratrol—cellular senescence—cancer

Cell senescence is a complex process that modifies the protein expression profile of cells and leads to replicative arrest and changes in metabolism, adhesion efficiency, and secretion phenotype (1). Cell senescence is accompanied by a striking increase in the secreted levels of approximately 40 factors involved in intercellular signaling, termed the "senescence-associated secretory phenotype" (SASP) (2). Cellular senescence response is considered an efficacious tumor suppressive mechanism, preventing at-risk cells, such as DNA damaged (3) cells, from undergoing malignant transformation. Some SASP components may reinforce these positive senescence features; however, when chronically present, SASP may be deleterious, stimulating age-associated tissue degeneration or creating a tumor-favoring tissue microenvironment, which promotes malignant phenotypes in vitro and in vivo [see reviews by Campisi and colleagues (4,5)]. SASP includes factors that may activate receptors and signaling pathways of neighbor cells and can be divided into the following three categories: (i) soluble signaling factors (interleukins, chemokines, and growth factors), (ii) secreted proteases, and (iii) insoluble components. The SASP mediators relevant for protumoral activity are as follows: (i) inflammatory cytokines, affecting both endothelial and epithelial cells (6) by activating the nuclear factor kappa-light-chain-enhancer of activated B cells (NF-kB) pathway (7) and inducing epithelial-mesenchymal transition (EMT) (4); (ii) members of CXCL and CCL families like IL-8, growth related

oncogene-alpha (GROα) and β, stromal derived factor1 (SDF1) and its receptor CXCR4 (8); (iii) matrix metallo-proteinases (MMPs) that alter the extracellular matrix (6) and have been showed to support mitogenic and chemotactic signal access to breast cancer cells (4); (iv) urokinase-plasminogen-activator/urokinase-plasminogen-activator receptor (uPA/uPAR) system (9,10); (v) almost all insulin-like growth factor (IGF)-binding proteins and their regulators (6). In addition, SASP-expressing senescent cells can exacerbate tumor immunoediting and eventually allow for the growth of immune-resistant cancer cells (11).

Fibroblasts are the main components of tissue stroma and their products are essential for remodeling and repair processes, but when activated or once senescent, they can contribute to progression and invasion of cancer cells, which is partially due to certain pro-inflammatory SASP factors, such as IL-6, IL-8, and GROα (12). Additionally, cancer-associated fibroblasts show a secretory pattern resembling SASP (10). This is the rationale for targeting senescent fibroblasts in tumor stroma to increase the effectiveness of cancer therapy (13).

A wide range of activities has been conferred to polyphenols, which are capable of modulating factors that are altered during aging and are relevant for age-related diseases. Polyphenols are widely distributed among dietary fruits and vegetables; their consumption has been related to a decreased risk of cardiovascular, metabolic, and neurodegenerative diseases, as well as cancer. Certain compounds, such as curcumin, epigallocatechin, and resveratrol, have been proposed as potential anticancer therapeutics, alone or in combination with classical chemotherapy, by interacting with multiple signaling pathways, including the NF-kB pathway. These compounds also modulate cell cycle and apoptosis (targeting p53 and the anti-apoptotic bcl-2 family members) and angiogenesis (targeting VEGF and FGF) [all reviewed by Fantini and colleagues (14)].

Among the polyphenolic compounds, resveratrol (*trans*-3,4,5-trihydroxystilbene) has been widely studied for its anti-senescence and anti-tumor properties (15), which are related to sirtuin1 activation and anti-oxidant features. Recently, resveratrol was reported to inhibit, through the above cited pathways, EMT in prostate, ovarian, and colorectal cancers as well as to synergize with tamoxifen in antiestrogen-resistant breast cancer cells (16).

Previous studies conducted in our lab (17,18) evaluated the effects of a long-term treatment (5 weeks) with low resveratrol concentrations (1 and 5 μM) in human MRC5 fibroblasts, a well-known in vitro senescence model. These concentrations are compatible with those attainable in vivo and are fairly maintained in culture (17). The treatment reverted some senescence-related morphologic and functional alterations in presenescent MRC5 cells (17) as well as inhibited gene expression and secretion of some SASP-related inflammatory molecules (18). In the present study, we used the forementioned chronic treatment with 5 μM resveratrol (reported as R5) of presenescent MRC5 fibroblast cultures progressing toward replicative senescence, to modulate the expression and release of SASP factors.

It is well-known that transforming growth factor-β1 (TGFβ1) mediates fibroblast activation to myofibroblasts (19), playing a central role in the development of a protumoral microenvironment. Additionally, the effect of R5 treatment on MRC5 fibroblast activation by TGFβ1 was evaluated. Furthermore, to mimic an anti-tumor hosting microenvironment in vitro, conditioned media (CM) from pretreated fibroblast cultures were used to assay their ability to modulate tumor-related phenotypes of A375 and A375-M6 melanoma cell lines.

Methods

Cell Cultures and Treatments

The MRC5 cell line is a normal human fibroblast cell line derived from fetal lung, and it was purchased from National Institute of Aging Cell Repository (Coriell Institute). The A375 human melanoma cell line (MITF wild type, BRAF V600E, NRAS wild type) was obtained from American Type Culture Collection (Manassas, VA), and A375-M6 melanoma cells were isolated from lung metastasis of SCID bg/bg mice that were i.v. injected with A375 and gently provided by Prof. Calorini (University of Florence). MRC5 fibroblasts and melanoma cells were cultured in high-glucose (4,500 mg/L) Dulbecco's Modified Eagle's Medium (DMEM, Euroclone) that was supplemented with 10% fetal bovine serum (FBS, Sigma–Aldrich), 2 mM l-glutamine, 100 units/mL penicillin, and 100 μg/mL streptomycin (Sigma–Aldrich) at 37°C in a 5% CO_2 humidified atmosphere. Cells were propagated at confluence by trypsinization.

The experiments on MRC5 fibroblasts were conducted on presenescent cultures, defined as having undergone more than 45 population doubling level (PDL). After chronic treatment for 5 weeks with or without 5 μM final resveratrol concentration (Sigma–Aldrich) and propagation in culture, with medium changes every 2 days, presenescent cells became senescent, as described previously (17,18). At the end of the treatment, control and resveratrol-treated senescent MRC5 cultures were named and reported as sen and senR5, respectively. Low PDL (<30) MRC5 fibroblasts were also propagated in culture and reported as young.

In some experiments, at the end of the 5-week treatment, sen and senR5 cell cultures were subsequently incubated for 24 hours in fresh DMEM added with transforming-growth-factor-beta 1 (TGFβ1, PeproTech) at a concentration of 10 ng/mL.

Preparation of MRC5 CM

At the end of treatments, cell cultures were washed with fresh PBS, next CM were collected after 24 hours of incubation with DMEM plus 2% FBS, and centrifugation at 1,500 rpm for 5 minutes. The medium volume/cell number proportion was 1 mL/1 × 10^5 MRC5 fibroblasts.

A375 and A375-M6 Treatment With MRC5 CMs

Melanoma cells were seeded at density of 2.0 × 10^4 cells/cm^2; once grown to approximately 80% confluency cells were incubated for 48 hours with unconditioned DMEM plus 2% FBS, reported as DMEM, or with CM from sen and senR5 MRC5. Then, cells were recovered by trypsinization for real time PCR (RT PCR), Western blot analyses, or invasion assays. Media for zymographies were collected from A375 and A375-M6 cultures that were susequently incubated for 24 hours with fresh unconditioned DMEM. The medium volume/cell number proportion was 1 mL/1.5 × 10^6 cells.

A375 and A375-M6 Growth Determination

Melanoma cells were seeded at a density of 2 × 10^4 cells/cm^2 and incubated with either DMEM or CM from either sen or senR5 fibroblasts. At 24, 48, and 72 h, cells were recovered by trypsinization and counted in a Bürker chamber. Cell viability was assessed by the Trypan Blue exclusion test.

Real Time PCR

Total RNA extraction was conducted using TRIzol reagent (Invitrogen). RNA was reverse transcribed with an iScript cDNA

Synthesis Kit using random primers. mRNA expression of selected genes was assayed by real time PCR using the primers (IDT, TemaRicerca) listed in Table 1 (Supplementary Table 1). Quantitative RT PCR was performed with an Applied Biosystem 7500 Fast RT PCR System (Applied Biosystem) using a SYBR Green-based detection with the default PCR settings as follows: 40 cycles of 95°C for 15 seconds and of 60°C for 60 seconds. The "Delta-delta method" was used for comparing relative gene expression results with GAPDH as the housekeeping gene. Data were normalized to results obtained in young, untreated MRC5 (sen), or in melanoma cells incubated with fresh unconditioned DMEM with 2% FBS (in all cases, assumed as value 100%) and expressed as the means ± standard deviation (SD) of three experiments.

Western Blot Analyses

Cell aliquots of MRC5, A375, and A375-M6 cells were collected at the end of the respective treatments and lysed in RIPA buffer (25 mM Tris–HCl pH 7.6, 150 mM NaCl, 1% NP-40, 1% sodium deoxycholate, 0.1% sodium dodecyl sulfate, SDS) with 1% protease inhibitor Cocktail (Sigma–Aldrich Chemicals Co.) and disrupted by sonication (Microson XL-2000, Misonix). Lysates were clarified by centrifugation and supernatant collected and stored at −20°C. Protein content was estimated by the Bio-Rad DC protein assay kit. Protein aliquots (30–40 µg), were separated using 12% SDS-polyacrylamide gel electrophoresis (SDS-PAGE, NuPAGE, Novex; Invitrogen), transferred to nitrocellulose membranes (Millipore), blocked in 5% skim milk and incubated overnight with the following specific primary antibodies: mouse anti-tubulin (clone DM 1A, T 9026 Sigma–Aldrich Chemicals Co.), mouse anti-α-smooth muscle actin (α-SMA, clone 1A4, A2547, Sigma–Aldrich Chemicals Co.), rabbit anti-NF-kB (GTX102090, GeneTex, Irvine, CA), mouse anti-uPAR (10G7, sc-13522, Santa Cruz, Santa Cruz, CA) that recognizes the full-length uPAR, rabbit anti-transforming growth factor β-receptor 2 (TGFβ-R2, 3713, Cell Signaling), rabbit anti-phospho-p38 mitogen activated protein kinase (P-p38, 92156, Cell Signaling), rabbit anti-p38 (44–6846, Biosource), rabbit anti-phospho-extracellular signal–regulated kinase (P-ERK, p42/p44, 9101, Cell Signaling), rabbit anti-ERK-2 (sc-154, Santa Cruz), mouse anti-N-cadherin (N-cad, clone 6G11, Dako), and rabbit anti-CXCR4 (AB 1846, Millipore), followed by the suitable HRP-conjugated secondary antibodies (Sigma–Aldrich Chemicals Co.). All resulting immunocomplexes were visualized with an enhanced chemiluminescence ECL detection system (GE Healthcare) and quantified by ImageJ software (NIH).

Invasion Assay

Analyses were performed in Boyden chambers, with wells separated by 8 µm-pore size polycarbonate filters coated with Matrigel (50 µg/filter). In chemoinvasion experiments, 2×10^4 A375 and 10^4 A375-M6 melanoma cells were suspended in 200 µL of DMEM plus 2% FBS and placed in upper well toward 200 µL of either MRC5 CM or unconditioned DMEM plus 2% FBS (used as reference) which was placed in the lower well. In spontaneous invasion experiments, subconfluent A375 and A375-M6 cultures were incubated for 48 hours with DMEM or MRC5 CM. Next, 2×10^4 cells from A375 cultures and 10^4 cells from A375-M6 cultures of each incubation group were suspended in 200 µL of fresh DMEM plus 2% FBS, respectively, and placed in the upper wells of Boyden chambers. Fresh DMEM plus 2% FBS was also placed in the lower well.

In both experiment types, invasion was performed for 6 hours at 37°C in 5% CO_2, then filters were recovered and fixed in methanol. Noninvading cells on the upper surface of the filter were removed with a cotton swab while invasive cells that were adherent on the lower filter surface were stained and counted using a light microscope.

For the chemoinvasion assay, the results were expressed as the percentage of cells that migrated toward MRC5 CMs compared to those that migrated toward DMEM. For spontaneous invasion activity determination, results were reported as the percentage of melanoma cells that migrated after preincubation with MRC5 CMs compared to those that migrated after preincubation with DMEM.

Zymography

Aliquots (30 µL) of CM obtained as described above from MRC5, A375, and A375-M6 cultures were mixed with Tris–Glycine SDS Native Sample Buffer (Invitrogen), electrophoresed through 10 % Novex Zymogram Gelatin Gels (Invitrogen) and developed according to the manufacturer's instructions. The bands containing gelatinolytic activity of MMP2 and MMP9 appeared transparent and were evident in the otherwise homogeneous blue gel. Bands were quantified using ImageJ software.

Statistical Analysis

Statistical analyses of the data were performed using one-way ANOVA, $p \leq .05$ was considered to be a statistically significant difference, and $p \leq .01$ was considered to be a very significant difference.

Results

Effect of Senescence on SASP-Related Factors Produced by MRC5 Fibroblasts

MRC5 fibroblasts, either at low (young) or high (sen) PDL levels, were analyzed for the expression of a group of genes related to SASP. Figure 1A shows the results of real time PCR experiments for IL1α; IL1β; chemokine TGFβ; proteases MMP2 and uPA; and receptors uPAR, TGFβ-R2, and CXCR4. The expression of all reported genes, except for TGFβ-R2, resulted significantly increased in sen MRC5. IL-1α was more than sevenfold upregulated in sen versus young MRC5 fibroblasts. A striking upregulation of CXCR4, with an approximately fourfold increase of uPA and TGFβ, and twofold uPAR mRNA levels were measured in sen compared to young fibroblasts.

Effect of Chronic Resveratrol Treatment on SASP-Related Factors Produced by MRC5 Fibroblasts

Presenescent MRC5 fibroblast cultures (PDL > 45) were treated for 5 weeks for replicative senescence (see Methods section), without (sen) and with (senR5) 5 µM resveratrol concentration (17,18).

Figure 1B shows the results of real time PCR experiments on the expression of SASP-related interleukins IL1α, IL1β, IL6, and IL8; chemokine TGFβ; proteases MMP3, MMP2 and uPA; and receptors uPAR, IL6R, IGF-1R, TGFβ-R2, and CXCR4. In treated MRC5 fibroblasts (senR5), IL1α, IL1β, IL6, and IL8 expression levels were reduced to 60%, 36%, 54%, and 95% of the basal levels (untreated cultures, sen), respectively. Gene expression levels of matrix metallo-proteinases MMP2 and MMP3 and serine protease uPA were found decreased to approximately 60%, which was accompanied by a reduction in the mRNA levels of the uPAR, IL6R, IGF-1R, TGFβ-R2 receptors, with the strongest effect on CXCR4 expression. Zymogram analysis (Figure 1C) of 24 hour CM, collected after resveratrol treatment (senR5), revealed a 30% reduction in the MMP2 active protein secretion, while MMP9 was almost unaffected

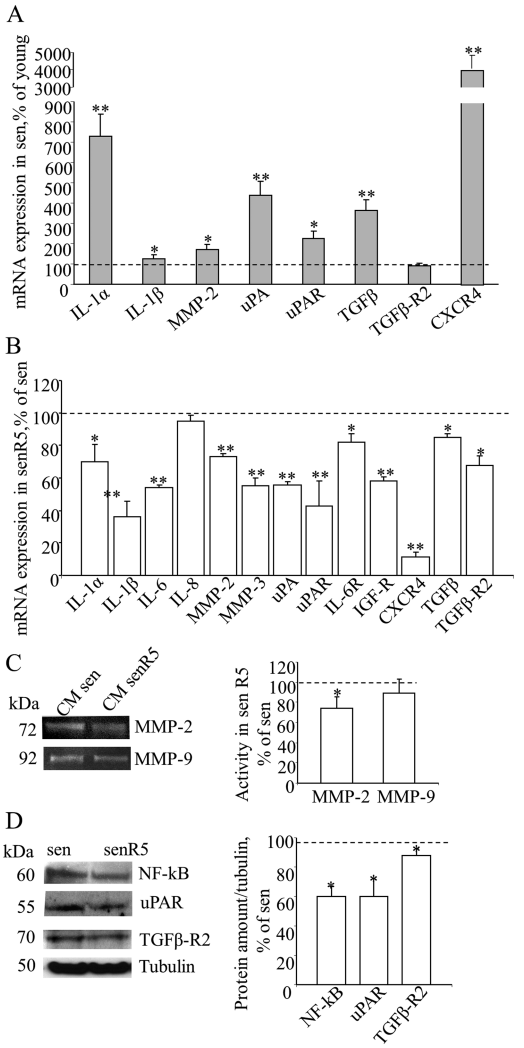

Figure 1. MRC5 senescent phenotype and effect of resveratrol treatment on gene expression and secretion of MRC5 SASP-related factors. (**A**) MRC5 fibroblasts, either at low (young) or high (sen) PDL levels, were analyzed for the expression of a group of genes related to SASP by Quantitative RT PCR, using GAPDH as the housekeeping gene. Histograms represent sen culture values normalized to young cultures (assumed as value 100% and indicated as the dot line) according to $2^{-\Delta\Delta C_t}$ method. * shows statistical significance ($p < .05$), ** show a very statistical significance ($p < .01$) compared to young. (**B**) Pre-senescent MRC5 fibroblast cultures were treated for 5 weeks in the absence (sen) or in the presence (senR5) of 5 μM resveratrol and analyzed by quantitative RT PCR for expression of indicated SASP-related genes. Data were reported as senR5 mRNA values normalized to untreated culture results (sen, assumed as value 100% and indicated as the dot line) according to $2^{-\Delta\Delta C_t}$ method and using GAPDH as the housekeeping gene. **(C)** Zymogram analysis of MRC5 conditioned media (CM). After 5 weeks of treatment, sen and senR5 cultures were incubated for 24 hours in DMEM in order to obtain CM. MMP-2 and MMP-9 activities were detected by gelatin zymography analysis as transparent bands (shown on the left) and quantified by ImageJ; histograms represent MMP-2 and MMP-9 activity measured in CM from R5 treated senescent fibroblasts (senR5) and referred as a percentage of values obtained in CM from untreated cultures (sen, dot line). Results represent the mean of three different experiments ± SD. (**D**) Western blot analyses of NF-kB, uPAR, TGFβ-R2 protein amounts in sen and senR5. Bands (shown on the left) were quantified by ImageJ; histograms represent the mean of the protein concentration detected in three different experiments ± SD. Data were normalized to untreated cultures (sen, assumed as value 100% and indicated as the dot line) and reported as a percentage. Tubulin was used as a loading control. In B, C, and D * shows statistical significance ($p < .05$), ** show a very statistical significance ($p < .01$) between senR5 and sen.

compared to control CM from untreated cultures (sen). Western blot analyses (Figure 1D) of senR5 cell extracts, compared to sen, showed reduced protein levels of NF-kB, uPAR (to approximately 60%, both), and TGFβ-R2 (to approximately 85%).

Effect of Chronic Resveratrol Pretreatment on MRC5 Activation by TGFβ

SenR5 and sen fibroblast cultures were incubated for 24 hours with or without 10 ng/mL TGFβ1 (see Methods section); then, cell extracts underwent to Western blot analyses. For zymogram analyses, CM were obtained in parallel cell cultures after TGFβ1 treatment, for 24 hours in DMEM plus 2% FBS, as reported in the Methods section.

Figure 2A shows that TGFβ1 treatment of senescent cultures (sen + TGFβ1) induced a fourfold increase in the cellular alpha-smooth actin (alpha-SMA) protein level. Resveratrol pretreatment was effective in reducing the sen fibroblast activation by TGFβ1. In fact, in senR5 + TGFβ1 cell extracts, the alpha-SMA protein concentration decreased the levels to near those of unstimulated cultures (sen).

Accordingly, zymogram analysis (Figure 2B) of CM after TGFβ1 treatment showed a significant increase in the MMP2 activity (sen +

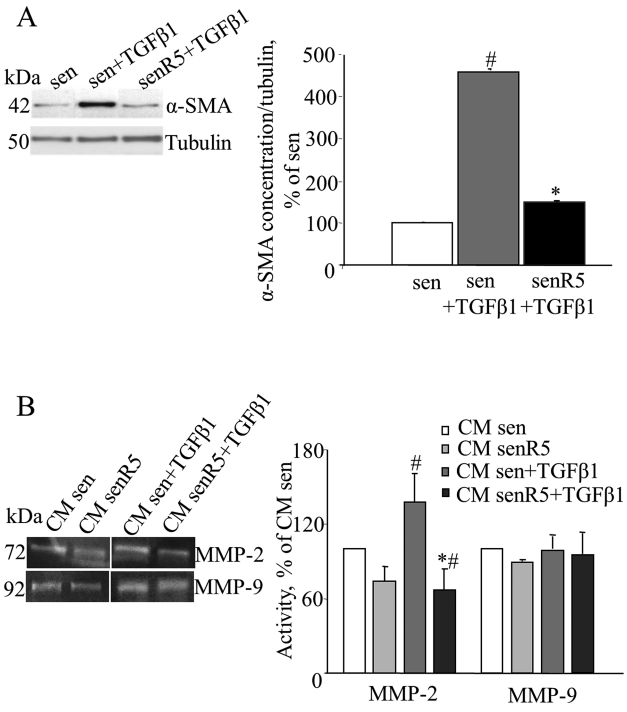

Figure 2. Resveratrol chronic pretreatment inhibits MRC5 fibroblast activation by TGFβ1. Presenescent MRC5 fibroblasts were treated for 5 weeks without (sen) or with (senR5) 5 μM resveratrol, then were incubated for 24 hours with 10 ng/mL TGFβ1. (**A**) Western blot analysis of α-SMA protein concentration. Bands (shown on the left) were quantified by ImageJ; histograms represent the mean of the protein levels detected in three different experiments ± SD. Results, reported as a percentage, were normalized to values obtained in sen, assumed as 100%. Tubulin was used as loading control. (**B**) Zymogram analysis of 24-hour CM harvested in sen and senR5 after TGFβ1 stimulation. Gelatinolytic activity was detected by zymogram analysis as transparent bands (shown on the left) and quantified by ImageJ; histograms show MMP-2 and MMP-9 activity in CM from sen and sen R5 without or with TGFβ1 stimulation. Results, reported as a percentage, represent the mean of three different experiments ± SD and are normalized to data obtained in CM from sen cultures that were not submitted to TGFβ1 stimulation (assumed as value 100%). * shows statistical significance ($p < .05$), between sen + TGFβ1 and senR5 + TGFβ1, # shows statistical significance ($p < .05$) compared to sen.

TGFβ1 vs sen). R5 preincubation of sen cultures revealed a significant reduction in the MMP2 activity, both with (CM senR5 + TGFβ1 vs CM sen + TGFβ1) and without (CM senR5 vs CM sen) stimulation by TGFβ1. Moreover, R5 pretreatment of TGFβ1 stimulated sen cultures induced CM levels of MMP2 activity that were even lower than those of sen unstimulated cells (CM senR5 + TGFβ1 vs CM sen). By contrast, MMP9 activity did not increase with TGFβ1 treatment and was almost unaffected by R5 pretreatment.

Effect of CM From MRC5 Fibroblasts on the Invasive Activity of A375 and A375-M6 Melanoma Cells

CM obtained from low PDL (<30) MRC5 cultures (CM young), together with media obtained from high PDL MRC5 cultures, either untreated (CM sen) or chronically pretreated with 5 μM resveratrol (CM senR5), were used for the experiments with A375 (Figure 3A and B) and A375-M6 (Figure 3C and D) melanoma cells. Additionally, fresh DMEM plus 2% FBS (DMEM) was used as a reference condition.

Chemoinvasion experiments were performed as described in the Methods section. Briefly, melanoma cell suspensions were placed in upper chambers of Matrigel-coated Transwell cell culture chambers and different CM were added to the lower chambers. After 6-hour incubation at 37°C, cells that had passed through the lower surface of the filter were photographed (Supplementary Figure 1) and counted; then, results were reported as histograms. CM from sen MRC5 cultures stimulated the invasion of A375-M6 cells (panel C), with approximately 70% and 50% increases in the migrated cell numbers compared to those that migrated toward DMEM, and toward CM young, respectively. CM from senR5 fibroblasts reduced the invasiveness of melanoma A375-M6 cells more than 40% compared to cells that migrated toward CM sen, reaching the levels obtained with young fibroblast CM. Additionally, A375 cell migration (panel A) was slightly, but significantly increased by CM from sen fibroblasts, and when CM from senR5 fibroblasts was placed in the lower chamber, the number of migrated cells was decreased to values approximately 50% of the values measured toward either unconditioned DMEM or CM young. In spontaneous invasion experiments (see photos in Supplementary Figure 1), subconfluent A375 and A375-M6 cultures were incubated for 48 hours with CMs obtained from young, sen and senR5 fibroblast cultures. Melanoma cells were then collected, counted, suspended in DMEM medium containing 2% FBS and seeded in the upper chamber of Matrigel-coated Transwell, as described above, except for the presence of standard DMEM plus 2% FBS in all lower chambers. After 6-hour incubation at 37°C, the spontaneous invasive activity of A375-M6 (panel D) melanoma cells after incubation with CM sen resulted in increases of 30% and 40% compared to unconditioned DMEM and to young fibroblast CM, respectively. The preincubation with CM senR5 was capable of reducing the A375-M6 spontaneous invasive activity to approximately 50%, compared to incubation with CM sen, and to levels slightly lower than those that were measured after incubation with CM young. No significant differences were measured in the spontaneous invasive activity of A375 melanoma cells (panel B).

Effects of CM From MRC5 Fibroblasts on the Growth and EMT Phenotype of A375 and A375-M6 Melanoma Cells

In these experiments, A375 and A375-M6 cultures were maintained for 72 hours with the above described MRC5 CM, namely

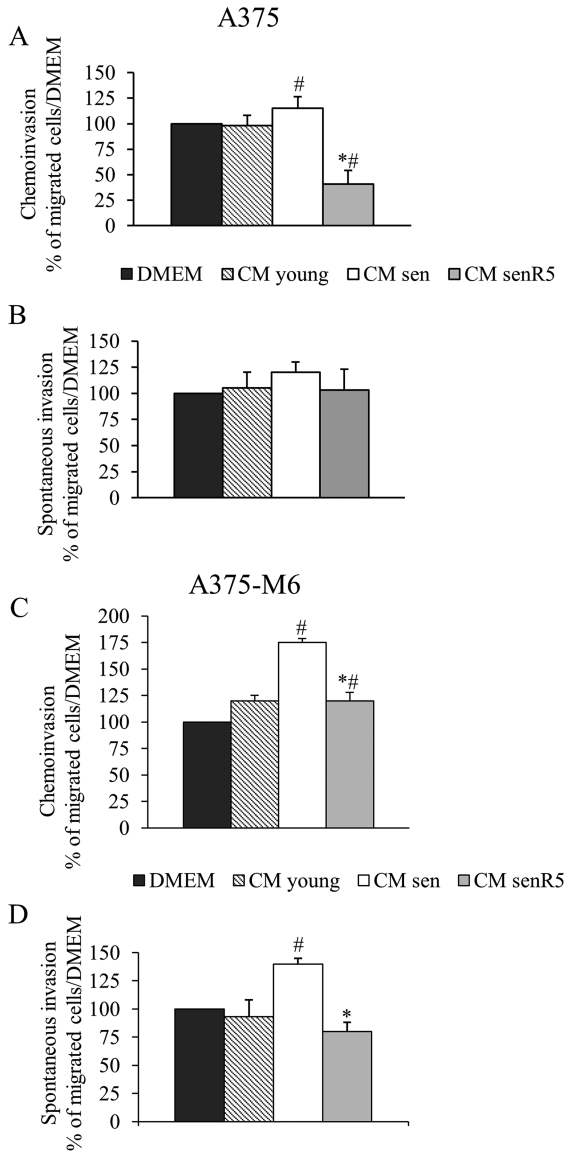

Figure 3. Effect of CM from MRC5 on A375 and A375-M6 cell invasion. 24 hour-CM from young fibroblasts (CM young) and from senescent cultures, either untreated (CM sen) or treated (CM senR5) for 5 weeks with 5 μM resveratrol were used in invasion experiments. Invasion test was performed with 2 × 10^4 A375 and 10^4 A375-M6 cells, for 6 hours at 37°C. **(A, C)** Matrigel chemoinvasion. A375 (A) and A375-M6 (C) melanoma cells were placed in the upper well while CM from young, sen and senR5 fibroblasts were placed in the lower one. Fresh DMEM was used as a reference condition. Histograms represent the mean of three different experiments ± SD, results are reported as a percentage of the migrated cells toward CM young, CM sen, or CM senR5, compared to those that migrated toward fresh DMEM (assumed as value 100%).* shows statistical significance ($p < .05$) compared to CM sen. # shows statistical significance ($p < .05$) compared to unconditioned DMEM. **(B, D)** Spontaneous invasion. A375 (B) and A375-M6 (D) melanoma cells were incubated for 48 hours with CM young, CM sen, CM senR5, or unconditioned DMEM (used as a reference condition). After incubation, melanoma cells were suspended in fresh DMEM that was placed also in the lower well. Histograms represent the mean of three different experiments ± SD, results are reported as a percentage of the migrated cells after preincubation with MRC5 CM compared to those that migrated after preincubation with DMEM (assumed as value 100%). * shows statistical significance ($p < .05$) compared to preincubation with CM sen. # shows statistical significance ($p < .05$) compared to preincubation with DMEM. Representative photographs of invasion experiments are shown in Supplementary Figure 1.

CM sen, CM senR5, and unconditioned DMEM. Melanoma cells were counted after 24, 48, and 72 hours of incubation. All counted cells were viable (according to Trypan blue exclusion test, data not shown). At 48 hour, cells from parallel cell cultures were collected, and used to obtain cell protein extracts. Figure 4 shows that medium produced by sen fibroblasts was effective in promoting the growth of A375 melanoma cells (Figure 4A), and there was a 40% increase in the cell count at 48 hour-incubation. This was not observed in A375-M6 cells (Figure 4C), which, as expected, showed a higher growth rate compared to A375 cultures, and were found confluent at 72 hours in either DMEM or sen CM conditions. Incubation of both A375 and A375-M6 cells with CM from senR5 fibroblasts produced a time-dependent inhibition of tumor cell proliferation, reaching 30% of the A375-M6 cell number reduction at 48 hours, compared to both incubations with CM sen and with unconditioned DMEM. Incubation with senR5 CM showed a more pronounced effect on A375 cell growth, and there was a 50% reduction compared to basal DMEM conditions, and 60% compared to sen CM, both at 48 and 72 hours.

Western blot analyses (Figure 4B and D) show that incubation with CM sen, compared to incubation with DMEM, produced an approximately 30% increase in the p38 phosphorylation in A375-M6 cells, and almost fourfold increase in the P-Erk p42 in both cell lines. In A375 cells, nearly 40% increase in the P-erk p44 was measured, and it was approximately fourfold increased upon sen CM incubation of A375-M6, compared to incubation with DMEM. All phosphorylated forms of p38 and Erk1/2 were negatively modulated in both A375 and A375-M6 melanoma cells that were incubated with CM senR5, and there was a striking reduction of P-p38, reaching levels that were 60% lower than incubation with unconditioned DMEM.

Figure 5 shows the results of mRNA expression for a panel of EMT-related genes, measured by RT PCR in either A375 (panel A) or A375-M6 (panel D) cells after 48-hour incubation with different CMs, as described above and reported as a percentage of results after incubation with unconditioned DMEM (indicated by the dot line at 100%). A significant increase in SDF1/CXCR4, and vimentin expression levels was measured in A375 melanoma cells that were incubated with CM sen compared to unconditioned DMEM incubation. In addition to the above reported genes, expression levels of uPA/uPAR and N-cad were significantly reduced by senR5 CM incubation compared to both CM sen and unconditioned DMEM conditions. Among the analyzed genes, a significant increase in the CXCR4, MMP2, uPA/uPAR, and N-cad expression levels was measured in A375-M6 melanoma cells incubated with CM sen compared to unconditioned DMEM incubation. By contrast, incubation of A375-M6 with CM senR5 determined a reduced expression of all genes compared to levels measured after incubation with CM sen. Expression of SDF1/CXCR4, uPA/uPAR, N-cad, Vimentin (VIM), and MMP9 was markedly reduced to the same or even lower levels than after incubation with unconditioned DMEM. Accordingly, Western blot analyses of melanoma cell extracts (panel B and E) for receptor proteins CXCR4 and uPAR, and for N-cad, confirmed the RT PCR results. In addition, uPAR and N-cad protein levels were strongly reduced by CM senR5 compared to CM sen and DMEM, while the effect on CXCR4 protein was less than anticipated from the RT PCR results.

Twenty-four–hour CM samples produced by A375 and A375-M6 cultures, were collected after a 48-hour preincubation with DMEM or CM from sen and senR5 fibroblasts and submitted to zymography (panel C and F) to detect MMP2 and MMP9 activity.

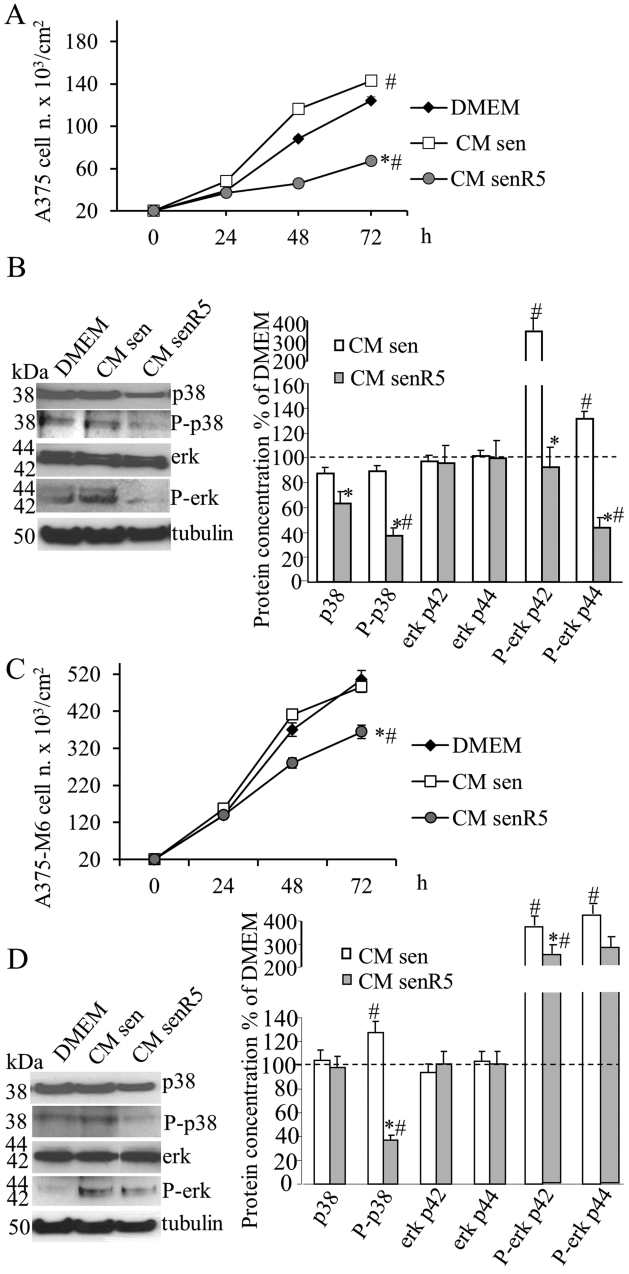

Figure 4. Effect of CM from MRC5 on the cell growth and kinase phosphorylation of A375 and A375-M6. Melanoma cells were seeded (2×10^4 per cm^2) and incubated with CM from sen, senR5 fibroblasts, or unconditioned DMEM. After 24, 48, and 72 hours of incubation with CM, A375 (**A**) and A375-M6 (**C**) melanoma cells were counted in a Bürker chamber. Cell viability was assessed by the Trypan Blue exclusion test. Results were expressed as the mean of three different experiments ± SD. * shows statistical significance ($p < .05$) compared to incubation with CM from sen fibroblasts, # shows statistical significance ($p < .05$) compared to incubation with DMEM. Western blot analyses of p38, P-p38, erk42/44 and P-erk 42/44 protein concentration in A375 **(B)** and A375-M6 (**D**) cells after 48 hours incubation with CM from sen and senR5 fibroblasts or with unconditioned DMEM. Tubulin was used as a loading control. Bands (shown on the left) were quantified by ImageJ; histograms represent the mean of protein concentrations of three different experiments ± SD. Results, reported as a percentage, were normalized to values obtained after incubation with unconditioned DMEM (assumed as value 100%, dot line). * shows statistical significance ($p < .05$) compared to incubation with CM from sen fibroblasts. # shows statistical significance ($p < .05$) compared to incubation with DMEM.

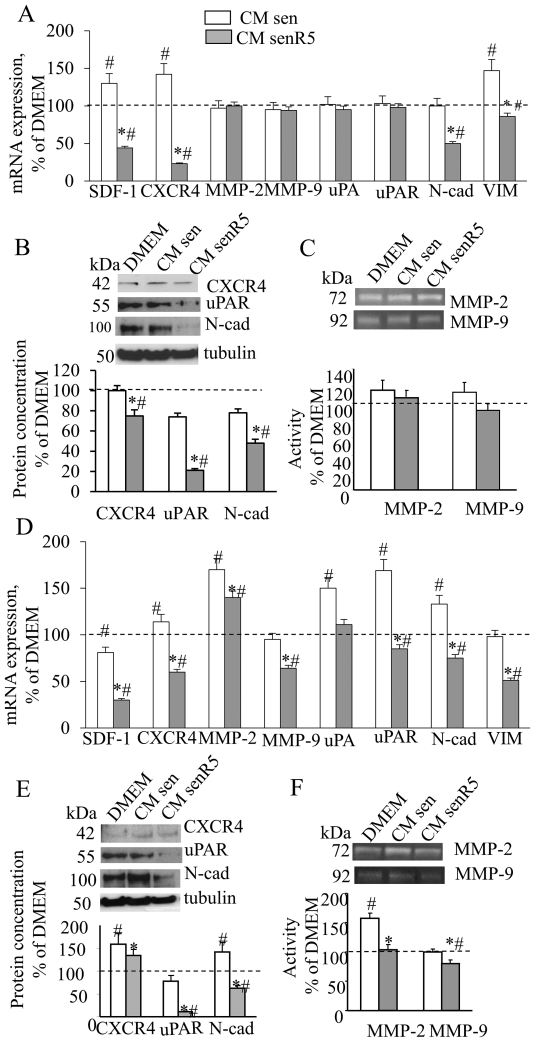

Figure 5. Effect of CM senR5 on EMT phenotype of A375 and A375-M6 melanoma cells. Cell cultures were incubated for 48 hours with CM from sen, senR5 fibroblasts, or unconditioned DMEM. (**A, D**) Quantitative RT PCR of EMT-related gene expression. Results (shown in histograms) are reported as a percentage of values obtained according to $2^{-\Delta\Delta C_t}$ method in A375 (A) and A375-M6 (D) melanoma cells after incubation with unconditioned DMEM (assumed as value 100%, dot line) and represent the mean of three different experiments ± SD. GAPDH was used as the housekeeping gene. * shows statistical significance ($p < .05$) compared to incubation with CM from sen fibroblasts. # shows statistical significance ($p < .05$) compared to incubation with DMEM. (**B, E**) Western blot analyses of CXCR4, uPAR, and N-cad protein concentration in A375 (B) and A375-M6 (E). Bands (shown on the top) were quantified by ImageJ; histograms represent the mean of the protein amount of three different experiments ± SD. Results were reported as a percentage and were normalized to values obtained after melanoma cell incubation with unconditioned DMEM (assumed as value 100%, dot line). Tubulin was used as a loading control. (**C, F**) Zymogram analyses of 24-hour CM harvested in A375 (C) and A375-M6 (F) after 48-hour preincubation with CM from sen, senR5 fibroblasts, or unconditioned DMEM. MMP-2 and MMP-9 activities were detected by gelatin zymography analysis and appeared as transparent bands (shown on the top). ImageJ was used for quantification. Histograms represent the mean of the gelatinolytic activity of melanoma CM measured in three different experiments ± SD. Results are reported as a percentage of values obtained after preincubation with unconditioned DMEM (assumed as value 100%, dot line). * shows statistical significance ($p < .05$) and ** show a very statistical significance ($p < .01$), compared to incubation with CM from sen fibroblasts. # shows statistical significance ($p < .05$) compared to incubation with DMEM.

No significant differences were measured in A375 melanoma cells (panel C). After preincubation with CM sen, only MMP2 activity was increased in CM produced by A375-M6 (panel F) melanoma cells, reaching values that were approximately 50% higher than the basal levels. Both gelatinolytic activities were reduced by preincubation with CM senR5, and with MMP2 reduced back to basal levels and MMP9 was reduced to lower than the basal levels.

Discussion

The ability of senescent human fibroblasts to promote carcinogenesis has been described and related to SASP factors in several papers by Campisi and colleagues (2,4–6,11,12,20,21). Cell senescence is a consequence of telomeric dysfunction related to repeated cell division (22); in addition, it is also a response to genotoxic stresses induced by anti-cancer therapeutic interventions, such as X-irradiation or chemotherapy (23). Recently, induction of senescence has been employed as a therapeutic approach in various tumors, including melanoma (24). At the same time, adverse effects produced by cellular senescence were measured and ascribed to SASP (25). Thus, in developing anti-cancer treatments, it might be necessary to develop adjuvant therapies targeting the cancer-promoting SASP, and at the same time maintaining the beneficial features of cell senescence (26,27).

We have previously reported that, in senescent MRC5 fibroblasts, the R5 treatment protocol induces a reduction in the expression levels and release of inflammatory IL6 and IL8, as well as of growth factors GROα and VEGF (18), which are responsible for inducing EMT and proliferation in both epithelial and endothelial cells (4). In this study, our senescent fibroblast model was validated by results obtained comparing SASP expression levels in young versus senescent MRC5 cultures. Interestingly, IL-1α, reported to be a general regulator of senescence-associated IL-6/IL-8 secretion (28), has been found more than sevenfold upregulated in senescent fibroblasts along with the increase in MMP2 and TGFβ mRNA levels (fourfold increased), and a striking upregulation of CXCR4. We confirmed those previous published data (18) and evaluated further SASP factors that are potentially related to the protumoral activity of our senescence model. These included metallo-proteinases and uPA, enzymes that are involved in altering the ECM, as well as surface receptor molecules, such as uPAR, CXCR4, and TGFβ-R2. In this regard, the uPA/uPAR system is known to be involved in tumor-related processes, such as cell migration, proliferation, and angiogenesis (9,10,29), and the SDF1/CXCR4 axis is the major mechanism responsible for autocrine and paracrine regulation of metastatic cancer features, which are primarily related to cell homing and migration (8,30). The R5-induced decrease in mRNA expression levels was confirmed by zymogram analyses for MMP2 activity in CM produced by R5-treated senescent fibroblasts and by cellular protein levels of receptors uPAR and TGFβ-R2. Moreover, we observed a significant decrease in the cellular NF-kB protein level, a transcription factor that has yet been reported to play a pivotal role in inducing SASP (31). Our chronic resveratrol treatment inhibited the activation of MRC5 to myofibroblast when exposed to TGFβ1, which was also reported by Fagone and colleagues (32) in ex vivo human lung fibroblasts and by Olson et al. (33) in cardiac fibroblasts that were exposed to angiotensin II. Myofibroblasts secrete and activate TGFβ, establishing a self-sustained feedback, and autocrine TGFβ-signaling has been shown to drive myofibroblast differentiation during tumor progression (34). In this context, the inhibition of the TGFβ1 effect, together with the lower expression of TGFβ and TGFβ-R2 mediated by R5 treatment of MRC5 senescent fibroblasts,

might confer protection against signaling mediated stroma activation. Upon TGFβ1-stimulation, MMP2 production and release in the medium by senescent MRC5 was counteracted by R5.

Taken together, these findings indicate that R5 treatment was effective in suppressing the major SASP components in our MRC5 senescence model, even in a TGFβ-activated microenvironment.

Metastatic melanoma is the most aggressive form of skin cancer, and novel therapeutic approaches have been developed with inhibitors of the RAF/MEK pathways co-targeted strategies, to bypass the frequent development of chemo-resistance (35). In recent years, significant attention has been placed on nutraceuticals, due to their disease modifying activities (36). Recently, preclinical studies on phytochemicals, both alone and in combination with traditional cytotoxic and targeted therapies, yielded promising results on melanoma treatment [reviewed by Strickland et al. (37)]. Additionally, resveratrol showed a role in counteracting multidrug resistance, by simultaneously acting on diverse mechanisms, that are relevant in both cancer prevention and treatment (16). In the present article, to evaluate the effects of R5 treatment on the tumorigenic activity of senescent MRC5 secretion, CM were tested on two human melanoma cell lines: A375, a cell line carrying BRAF mutation (38) that is characterized by a low metastatic potential, and A375-M6 cells, a murine lung metastatic cell line derived from A375. Functional assays on the invasive properties of melanoma cells revealed a protumoral effect of CM produced by senescent MRC5, compared to both unconditioned medium and CM produced by low PDL, young MRC5 cultures. An increase in the invasiveness of both melanoma cell lines was measured when senescent CM was used as a chemo-attractant. This chemo-attractant was less effective for A375 melanoma than for A375-M6 cells when it was used in 48-hour pretreatment of cancer cells before the invasion test (reported as spontaneous invasion test). A375 and A375-M6 cells have been analysed for mRNA expression of genes that directly or indirectly could be related to the protumorigenic effect of CM from senescent MRC5. We found a significant increase in the expression of the EMT marker N-cad, of CXCR4, of uPA/uPAR system, and gelatinase MMP2, and all of these could be associated with the increase in melanoma cell invasiveness (39–42). The R5 treatment protocol was capable of reducing the deleterious effects induced by senescent CM on A375 and A375-M6 malignant features. Specifically, the treatment reduced the SDF1/CXCR4 axis, MMP2 protease activity, and uPA/uPAR system. In addition, it reduced EMT markers N-cad and Vim. All of these molecular changes most likely underlie the concomitant reduction in melanoma invasiveness.

The mitogen-activated protein kinase (MAPK) signaling pathway is associated with cell differentiation, proliferation, and survival. Four MAPK cascades have been identified, ERK1/2, c-Jun N-Terminal kinase (JNK), p38, and ERK5 cascades. In the present work, we found an increase in phosphorylation of both p38 and ERK1/2 after 48 hours of incubation of both A375 and A375-M6 melanoma cells with CM produced by senescent MRC5 fibroblasts, which further confirmed the protumoral activity of SASP. Conversely, the incubation with CM from R5-treated senescent cells was effective in reducing the phosphorylation levels of both proteins. The negative modulation of P-ERK1/2 could also account for the observed concomitant down-regulation of uPAR (43,44). Similar results were recently reported by Liu and colleagues (45) who used simvastatin to reduce senescent fibroblast SASP deleterious effects on breast cancer cell proliferation. Accordingly, the proliferation rate of melanoma cells was reduced by CM from R5-treated senescent cells. Given the correlation between the metastatic potential and proliferative activity of A375 melanoma cells (46), our results suggest that the regulation of SASP by R5 treatment might be useful for controlling A375 tumor progression, through inhibiting of A375 proliferation, together with the substantial decrease in EMT markers, SDF1/CXCR4 and uPA/uPAR systems.

Overall, senR5 CM had slightly different effects on the tumoral phenotype of A375 and A375-M6 melanoma cell lines. It was more efficacious in decreasing the growth-related phenotypes of A375 melanoma and it was not very effective against cell spontaneous invasion after treatment, which is probably due to the low basal metastatic potential of A375, but their migration toward senR5 medium was significantly reduced, confirming the anti-tumoral effect of R5 pretreatment on senescent fibroblast CM. However, senR5 CM incubation was capable of more efficiently reducing the spontaneous invasive activity of A375-M6 metastatic melanoma cells, indicating a possible effect in reducing their metastatic potential, which was also demonstrated by the decrease in MMPs gene expression and activities.

We can conclude that chronic resveratrol treatment might be a powerful strategy in counteracting the "dark side" of senescence without affecting the tumor suppressive mechanisms. In fact, we previously showed that R5 treatment did not extend the MRC5 lifespan (17) and did not modify the p16/INK4a expression (18) of senescent treated fibroblasts. The protective, anti-tumoral activity of CM from R5-treated senescent MRC5 fibroblasts might be due to a decrease in a wide-range of detrimental SASP factors.

This innovative experimental approach supports the development of preventive and anti-cancer treatments that target the stromal cell phenotype, which can indirectly modulate the neoplastic features of melanoma cells.

Supplementary Material

Supplementary data are available at *The Journals of Gerontology, Series A: Biological Sciences and Medical Science*s online.

Funding

This work was supported by funds from the University of Florence and from Associazione Italiana per la Ricerca sul Cancro (AIRC, IG 2013 N.14266).

Conflict of Interest

The authors declare that they have no conflict of interest to report.

References

1. Hwang ES, Yoon G, Kang HT. A comparative analysis of the cell biology of senescence and aging. *Cell Mol Life Sci*. 2009;66:2503–2524. doi:10.1007/s00018-009-0034-2
2. Coppé JP, Patil CK, Rodier F, et al. Senescence-associated secretory phenotypes reveal cell-nonautonomous functions of oncogenic RAS and the p53 tumor suppressor. *PLoS Biol*. 2008;6:2853–2868. doi:10.1371/journal.pbio.0060301
3. D'Adda di Fagagna F. Living on a break: cellular senescence as a DNA-damage response. *Nat Rev Cancer*. 2008;512–522. doi:10.1038/nrc2440
4. Davalos AR, Coppe JP, Campisi J, Desprez PY. Senescent cells as a source of inflammatory factors for tumor progression. *Cancer Metastasis Rev*. 2010;29:273–283. doi:10.1007/s10555-010-9220-9
5. Campisi J. Aging, cellular senescence, and cancer. *Annu Rev Physiol*. 2013;75:685–705. doi:10.1146/annurev-physiol-030212-183653
6. Coppé JP, Desprez PY, Krtolica A, Campisi J. The senescence-associated secretory phenotype: the dark side of tumor suppression. *Annu Rev Pathol*. 2010;5:99–118. doi:10.1146/annurev-pathol-121808-102144

7. Mantovani A, Locati M, Vecchi A, Sozzani S, Allavena P. Decoy receptors: a strategy to regulate inflammatory cytokines and chemokines. *Trends Immunol*. 2001;22:328–336. doi:10.1016/S1471-4906(01)01941-X
8. Chatterjee S, Behnam Azad B, Nimmagadda S. The intricate role of CXCR4 in cancer. *Adv Cancer Res*. 2014;124:31–82. doi:10.1016/B978-0-12-411638-2.00002-1
9. Del Rosso M, Fibbi G, Pucci M, Cerinic MM. Antisense oligonucleotides against the urokinase receptor: a therapeutic strategy for the control of cell invasion in rheumatoid arthritis and cancer. *Clin Exp Rheumatol*. 1998;16:389–393.
10. Blasi F, Carmeliet P. uPAR: a versatile signalling orchestrator. *Nat Rev Mol Cell Biol*. 2002;3:932–943. doi:10.1038/nrm977
11. Velarde MC, Demaria M, Campisi J. Senescent cells and their secretory phenotype as targets for cancer therapy. *Interdiscip Top Gerontol*. 2013;38:17–27. doi:10.1159/000343572.11
12. Krtolica A, Parrinello S, Lockett S, Desprez PY, Campisi J. Senescent fibroblasts promote epithelial cell growth and tumorigenesis: a link between cancer and aging. *Proc Natl Acad Sci U S A*. 2001;98:12072–12077. doi:10.1073/pnas.211053698
13. Elkhattouti A, Hassan M, Gomez CR. Stromal fibroblast in age-related cancer: role in tumorigenesis and potential as novel therapeutic target. *Front Oncol*. 2015;5:158. doi:10.3389/fonc.2015.00158
14. Fantini M, Benvenuto M, Masuelli L, et al. In vitro and in vivo antitumoral effects of combinations of polyphenols, or polyphenols and anticancer drugs: perspectives on cancer treatment. *Int J Mol Sci*. 2015;16:9236–9282. doi:10.3390/ijms16059236
15. Baur JA, Sinclair DA. Therapeutic potential of resveratrol: the in vivo evidence. *Nat Rev Drug Discov*. 2006;5:493–506. doi:10.1038/nrd2060
16. Varoni EM, Lo Faro AF, Sharifi-Rad J, Iriti M. Anticancer molecular mechanisms of resveratrol. *Front Nutr*. 2016;3:8. doi:10.3389/fnut.2016.00008
17. Giovannelli L, Pitozzi V, Jacomelli M, et al. Protective effects of resveratrol against senescence-associated changes in cultured human fibroblasts. *J Gerontol A Biol Sci Med Sci*. 2011;66:9–18. doi:10.1093/gerona/glq161
18. Pitozzi V, Mocali A, Laurenzana A, et al. Chronic resveratrol treatment ameliorates cell adhesion and mitigates the inflammatory phenotype in senescent human fibroblasts. *J Gerontol A Biol Sci Med Sci*. 2013;68:371–381. doi:10.1093/gerona/gls183
19. Yokozeki M, Moriyama K, Shimokawa H, Kuroda T. Transforming growth factor-beta 1 modulates myofibroblastic phenotype of rat palatal fibroblasts in vitro. *Exp Cell Res*. 1997;231:328–336. doi:10.1006/excr.1997.3473
20. Rodier F, Campisi J. Four faces of cellular senescence. *J Cell Biol*. 2011;192:547–556. doi:10.1083/jcb.201009094
21. Laberge RM, Sun Y, Orjalo AV, et al. MTOR regulates the pro-tumorigenic senescence-associated secretory phenotype by promoting IL1A translation. *Nat Cell Biol*. 2015;17:1049–1061. doi:10.1038/ncb3195
22. Harley CB, Futcher AB, Greider CW. Telomeres shorten during ageing of human fibroblasts. *Nature*. 1990;345:458–460. doi:10.1038/345458a0
23. Ewald JA, Desotelle JA, Wilding G, Jarrard DF. Therapy-induced senescence in cancer. *J Natl Cancer Inst*. 2010;102:1536–1546. doi:10.1093/jnci/djq364
24. Mo J, Sun B, Zhao X, et al. Hypoxia-induced senescence contributes to the regulation of microenvironment in melanomas. *Pathol Res Pract*. 2013;209:640–647. doi:10.1016/j.prp.2013.07.004
25. Bruyère C, Mathieu V, Vessières A, et al. Ferrocifen derivatives that induce senescence in cancer cells: selected examples. *J Inorg Biochem*. 2014;141:144–151. doi:10.1016/j.jinorgbio.2014.08.015
26. Dörr JR, Yu Y, Milanovic M, et al. Synthetic lethal metabolic targeting of cellular senescence in cancer therapy. *Nature*. 2013;501:421–425. doi:10.1038/nature12437
27. Lecot P, Alimirah F, Desprez PY, Campisi J, Wiley C. Context-dependent effects of cellular senescence in cancer development. *Br J Cancer*. 2016;114:1180–1184. doi:10.1038/bjc.2016.115
28. Orjalo AV, Bhaumik D, Gengler BK, Scott GK, Campisi J. Cell surface-bound IL-1alpha is an upstream regulator of the senescence-associated IL-6/IL-8 cytokine network. *Proc Natl Acad Sci U S A*. 2009;106:17031–17036. doi:10.1073/pnas.0905299106
29. Del Rosso M. uPAR in angiogenesis regulation. *Blood*. 2011;117:3941–3943. doi:10.1182/blood-2011-02-337733
30. Neagu M, Constantin C, Longo C. Chemokines in the melanoma metastasis biomarkers portrait. *J Immunoassay Immunochem*. 2015;36:559–566. doi:10.1080/15321819.2015.1035593
31. Salminen A, Kauppinen A, Kaarniranta K. Emerging role of NF-κB signaling in the induction of senescence-associated secretory phenotype (SASP). *Cell Signal*. 2012;24:835–845. doi:10.1016/j.cellsig.2011.12.006
32. Fagone E, Conte E, Gili E, et al. Resveratrol inhibits transforming growth factor-β-induced proliferation and differentiation of ex vivo human lung fibroblasts into myofibroblasts through ERK/Akt inhibition and PTEN restoration. *Exp Lung Res*. 2011;37:162–174. doi:10.3109/01902148.2010.524722
33. Olson ER, Naugle JE, Zhang X, Bomser JA, Meszaros JG. Inhibition of cardiac fibroblast proliferation and myofibroblast differentiation by resveratrol. *Am J Physiol Heart Circ Physiol*. 2005;288:H1131–H1138. doi:10.1152/ajpheart.00763.2004
34. Kojima Y, Acar A, Eaton EN, et al. Autocrine TGF-beta and stromal cell-derived factor-1 (SDF-1) signaling drives the evolution of tumor-promoting mammary stromal myofibroblasts. *Proc Natl Acad Sci U S A*. 2010;107:20009–20014. doi:10.1073/pnas.1013805107
35. Grazia G, Penna I, Perotti V, Anichini A, Tassi E. Towards combinatorial targeted therapy in melanoma: from pre-clinical evidence to clinical application (review). *Int J Oncol*. 2014;45:929–949. doi:10.3892/ijo.2014.2491
36. Nasri H, Baradaran A, Shirzad H, Rafieian-Kopaei M. New concepts in nutraceuticals as alternative for pharmaceuticals. *Int J Prev Med*. 2014;5:1487–1499.
37. Strickland LR, Pal HC, Elmets CA, Afaq F. Targeting drivers of melanoma with synthetic small molecules and phytochemicals. *Cancer Lett*. 2015;359:20–35. doi:10.1016/j.canlet.2015.01.016
38. Padua RA, Barrass N, Currie GA. A novel transforming gene in a human malignant melanoma cell line. *Nature*. 1984;311:671–673.
39. Bianchini F, D'Alessio S, Fibbi G, Del Rosso M, Calorini L. Cytokine-dependent invasiveness in B16 murine melanoma cells: role of uPA system and MMP-9. *Oncol Rep*. 2006;15:709–714. doi:10.3892/or.15.3.709
40. Siret C, Terciolo C, Dobric A, et al. Interplay between cadherins and α2β1 integrin differentially regulates melanoma cell invasion. *Br J Cancer*. 2015;113:1445–1453. doi:10.1038/bjc.2015.358
41. Mc Connell AT, Ellis R, Pathy B, Plummer R, Lovat PE, O'Boyle G. The prognostic significance and impact of the CXCR4/CXCR7/CXCL12 axis in primary cutaneous melanoma. *Br J Dermatol*.2016. doi:10.1111/bjd.14720
42. O'Boyle G, Swidenbank I, Marshall H, et al. Inhibition of CXCR4-CXCL12 chemotaxis in melanoma by AMD11070. *Br J Cancer.* 2013;108:1634–1640. doi:0.1038/bjc.2013.124
43. Khoi PN, Xia Y, Lian S, et al. Cadmium induces urokinase-type plasminogen activator receptor expression and the cell invasiveness of human gastric cancer cells via the ERK-1/2, NF-κB, and AP-1 signaling pathways. *Int J Oncol*. 2014;45:1760–1768. doi: 10.3892/ijo.2014.2558.
44. Brunner PM, Heier PC, Mihaly-Bison J, Priglinger U, Binder BR, Prager GW. Density enhanced phosphatase-1 down-regulates urokinase receptor surface expression in confluent endothelial cells. *Blood*. 2011;117:4154–4161. doi:10.1182/blood-2010-09-307694
45. Liu S, Uppal H, Demaria M, Desprez PY, Campisi J, Kapahi P. Simvastatin suppresses breast cancer cell proliferation induced by senescent cells. *Sci Rep*. 2015;5:17895. doi:10.1038/srep17895
46. Chandrasekaran S, Giang UB, Xu L, DeLouise LA. In vitro assays for determining the metastatic potential of melanoma cell lines with characterized in vivo invasiveness. *Biomed Microdevices*. 2016;18:89. doi:10.1007/s10544-016-0104-9